Global and Planetary Change 220 (2023) 104022

Contents lists available at ScienceDirect

Global and Planetary Change

journal homepage: www.elsevier.com/locate/gloplacha

Changing sediment supply during glacial-interglacial intervals in the North Atlantic revealed by particle size characterization and environmental magnetism

Stephanie Leone [a], Dan V. Palcu [a,b,*], Priyeshu Srivastava [a], Muhammad Bin Hassan [a], Joy R. Muraszko [a,c], Luigi Jovane [a]

[a] Instituto Oceanográfico, Universidade de São Paulo, São Paulo, Brazil
[b] Department of Earth Sciences, Utrecht University, the Netherlands
[c] Laboratory of Orogenic Belts and Crustal Evolution, School of Earth and Space Sciences, Peking University, Beijing, China

ARTICLE INFO

Editor: Dr. Fabienne Marret-Davies

Keywords:
DSDP Leg 94 Hole 611A
Early Pleistocene
Glacial-interglacial intervals
Paleoclimate
Sediment provenance
IRD

ABSTRACT

The Pliocene-Pleistocene transition is characterized by an abundance of Ice-Rafted Debris (IRD) in the North Atlantic basin. One of the regions affected by IRD during this period is the Gardar Drift, where the DSDP Leg 94 Hole 611A is located. This region received sediments from different sources during the glacial and interglacial intervals (e.g., Iceland and Greenland). We analyzed grain size and particle-size specific magnetic properties of sediments for their provenance characterization between ~2.64 and 2.52 Ma. Our results show that major proportion of bulk sediments during both glacial and interglacial periods were made up of basaltic-rich Icelandic sediments, whereas only during intense glacial periods (Marine Isotope Stages 100 and 104), a small proportion of non-basaltic sand compositions were identified, possibly sourced from Greenland and other non-basaltic provenance. The non-basaltic sand fractions during the intense glacial periods were likely supplied as IRDs. In addition, a new level of coarse lithics (38 pcs. of >1 mm) composed of different rocks types (e.g., basalt, granite, granodiorite etc.) were identified in DSDP 611A Hole during the end of MIS 104 glacial period. The coarse lithic fragments showed distinctive magnetic properties than rest of the particle sizes and were classified as Iceberg-Rafted Debris (IBRD). Overall, our results show that higher sand percentage was found during the intense glacial episodes, and their magnetic grain size analysis could help in distinguishing their provenance. We elaborate that particle size specific magnetic measurements of sand fractions could help in rapidly characterizing the glacial episodes in the subpolar North Atlantic.

1. Introduction

The continental glaciers in the Earth's Northern Hemisphere (Arctic and Greenland-Norwegian Sea regions) have existed since as early as in the Eocene-Oligocene (e.g., Eldrett et al., 2007; Stickley et al., 2009; Tripati and Darby, 2018). Ice-rafted debris (IRD) based records from the subpolar North Atlantic marine sediments suggested ice-shelf glaciations in the Greenland-Norwegian Sea regions since late Miocene (Jansen and Sjøholm, 1991; Larsen et al., 1994), however, major ice sheet development in the Northern Hemisphere was not present until the late Pliocene and earliest Pleistocene (~3.6–2.4 Ma) (Shackleton et al., 1984; Maslin et al., 1998; Kleiven et al., 2002). The IRD records from the subpolar North Atlantic showed intensification of Northern Hemisphere Glaciation (iNHG), as a synchronous expansion of continental icesheets in Greenland, Scandinavia and Northeast America, at ~2.72 Ma (Marine Isotope Stage G6) followed by waxing and waning of ice sheets during glacial–interglacial cycles in the Quaternary (Shackleton et al., 1984; Maslin et al., 1998; Kleiven et al., 2002; Hodell and Channell, 2016).

The iNHG has an irreversible effect on global climate and is associated with the pronounced cooling, significant fall in sea level (Droxler and Jorry, 2021; Rohling et al., 2014; Miller et al., 2020), weakened Atlantic Meridional Overturning Circulation (AMOC) (Raymo et al., 1992; Kleiven et al., 2002; Hassold et al., 2006; Dausmann et al., 2017), and increased input of continental terrigenous material in the subpolar North Atlantic (Hassold et al., 2006). Recently, Hayashi and Ohno (2021) suggested increased strength of AMOC during the late Pliocene,

* Corresponding author at: Department of Earth Sciences, Utrecht University, the Netherlands
E-mail address: d.v.palcu@uu.nl (D.V. Palcu).

https://doi.org/10.1016/j.gloplacha.2022.104022
Received 2 May 2022; Received in revised form 8 December 2022; Accepted 20 December 2022
Available online 22 December 2022

which amplified the iNHG.

The provenance of the glacio-fluvial terrigenous sediments from the subpolar North Atlantic can provide information on the spatial-temporal glacial extent as well as on the strength of oceanic circulations during the iNHG. To fingerprint the sediment sources several studies have been carried out on the late Pliocene and Quaternary subpolar North Atlantic sediments and IRD deposits using the methods of major element chemistry (e.g., Gruetzner and Higgins, 2010; Hodell et al., 2010), stable and radiogenic isotopes (e.g., DePaolo et al., 2006; Farmer et al., 2003; Bailey et al., 2012, 2013; Hemming et al., 1998), magnetic mineralogy and grain sizes (Stoner et al., 1995; Kanamatsu et al., 2009; Sato et al., 2015) and magnetic fabrics (Hassold et al., 2006). The subpolar North Atlantic consist of sediments (including IRD) removed by erosion from the surrounding landmasses, of which Iceland and Greenland are prime contributors (Prins et al., 2002; Hatfield et al., 2013), and to a lesser extent from Labrador, Scandinavia, and the British Isles (Bailey et al., 2012). Iceland (and Midwest of Greenland) rocks predominantly consist of tholeiitic basalt, transitional alkaline basalts and alkali olivine basalts of Paleogene and Neogene age (Ward, 1971; Jakobsson, 1972; Schilling et al., 1982). The clastic material from Greenland consists of Precambrian rocks and can be divided into three geological types: gneisses and granites from the Archean Block and Nagssygtoqdian Mobile Belt, and granitic rocks from the Ketilidian Mobile Belt, (Kalsbeek and Taylor, 1985). Other provenance areas are Newfoundland and Labrador to the West, and to a lesser extent provenance from the NE (Scotland, Ireland, and Scandinavia), regions with predominantly non-basaltic rock.

The Gardar drift is a large sedimentary drift deposit located in the subpolar North Atlantic region. The Gardar drift has been suggested to be the locus of IRD deposits during the intensified iNHG in the late Pliocene and earliest Pleistocene (Bailey et al., 2012, 2013). In the present work, we study physical grain size and magnetic properties of six different particle size fractions between sand and clay from the Gardar drift Deep Sea Drilling Project (DSDP) Site 611A, covering the iNHG time span between MIS G2 and 99 (~2.64 to 2.49 Ma) (Fig. 1).

A new approach was recently developed to characterize and distinguish the magnetic minerals of the Iceland and Greenland by analyzing the particle size specific magnetic properties of glacial-fluvial sediments collected near the Greenland and Iceland margins (Hatfield et al., 2013, 2017) as well as from the Norwegian-Greenland Seas (Hatfield et al., 2019). Moreover, coarse sand (2 mm and 250 μm) fraction is recently related to dynamic of the calving margins as iceberg rafted debris (IBRD) (Krissek, 1995; Wilson et al., 2018). The particle size specific magnetic analysis has shown that magnetic properties of the sediments from these regions have great dependency on the physical particle sizes. We applied this method on the samples from Gardar drift to identify the provenance of magnetic minerals during the glacial and interglacial. While the provenance of IRD deposits from the DSDP 611A based on Pb isotopic composition of coarse lithic feldspar is reported for the studied time interval in Bailey et al. (2012), physical grain size and particle specific magnetic analysis of sand, silt and clay fractions can provide additional information on the bulk sediment provenance, and surface and deep-water circulations. We show that the particle size specific magnetic analysis can help in distinguishing the sediment provenance of subpolar North Atlantic sediments during the glacial and interglacial, and rapid, non-destructive, and relatively economical method of environmental magnetism can be used effectively for such distinctive objectives.

2. Regional setting

Gardar Drift is a large contourite drift deposit, on the lower eastern flank of the Reykjanes Ridge (52°5′N; 30° 2′W), near the Charlie-Gibbs Fracture Zone, above influence of Norwegian Sea (Bianchi and McCave, 2000). It was formed by lateral transport of fine sediment material-brought by the southward flowing Iceland-Scotland Overflow Water (ISOW) bottom currents with NE-SW orientation [Ruddiman, 1977; Faugères et al., 1993; Wold, 1994; Bianchi and McCave, 2000]. The ISOW water mass is a mixture of Norwegian Sea Deep Water (NSDW) and Arctic Intermediate Water (AIA) (Bianchi and McCave, 2000; Blake-Mizen et al., 2019), and makes up 25% of North Atlantic Deep Water (NADW) (de Carvalho Ferreira and Kerr, 2017). The Gardar contourite drift is a prism that start at southwest near the Charlie-Gibbs Fracture Zone with a depth of 3000 m and develop towards northeast for about 1100 km up to a water depth of 1400 m. A depression approximately 200–300 m deep separates the Gardar Drift from the southern end of Björn Drift (Bianchi and McCave, 2000).

Geochemical and rock magnetic characteristics of bulk sediments (terrigenous fractions) of different time periods i.e., from late Pliocene to Holocene and on latitudinal gradient (N-S) of the Gardar drift have been previously investigated in several studies (e.g., Kissel, 2005, Kissel et al., 1999, 2009; Ballini et al., 2006; Gruetzner and Higgins, 2010; Sato

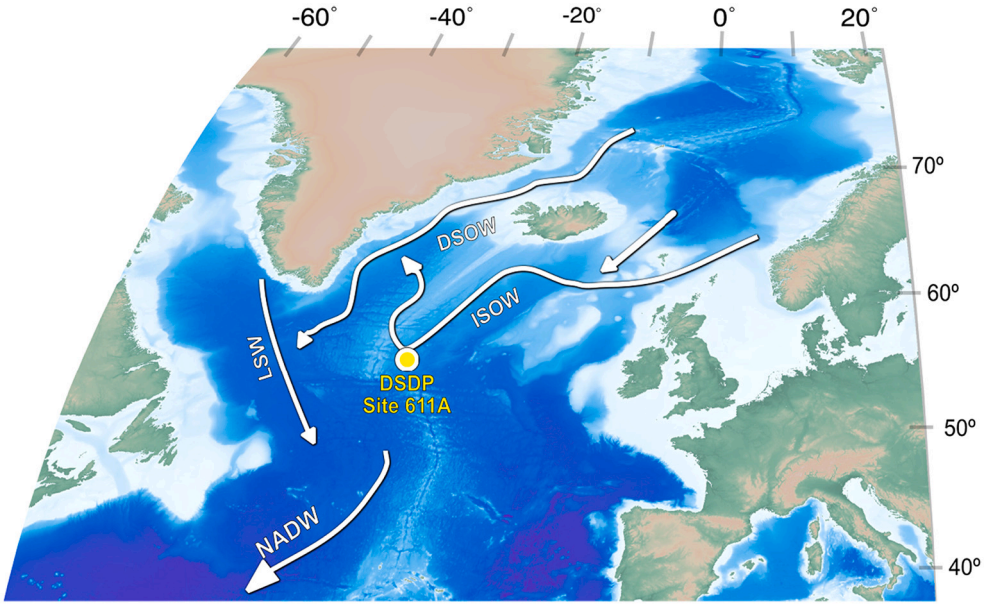

Fig. 1. Location of the DSDP Site 611A in the North Atlantic and ocean circulation patterns in the North Atlantic. Acronyms on map: NADW – North Atlantic Deep Water, LSW – Labrador Sea Water, DSOW – Denmark Strait Overflow, ISOW – Iceland-Scotland Overflow Water.

et al., 2015; Kanamatsu et al., 2009). In general, the terrigenous fractions in the Gardar drift are divided into the mafic basaltic fractions rich in titanium, and relatively acidic (felsic) sediments rich in potassium (Kissel et al., 2009; Ballini et al., 2006; Gruetzner and Higgins, 2010). The magnetic rich basaltic fractions in the Gardar drift are mainly sourced from the Iceland and the Faeroe Islands brought by southward flowing ISOW(Kissel et al., 2009; Ballini et al., 2006; Hayashi and Ohno, 2021). Whereas felsic sediments are sourced from the surrounding continental rocks either through ice-rafting during the glacial (stadials) (Ballini et al., 2006) and/or brought by Northeast Atlantic Deep Water (NEADW)/Lower Deep Water (LDW) when ISOW had shoaled (Gruetzner and Higgins, 2010). The magnetic rich basaltic fractions are generally higher in the Gardar drift during the interglacial (interstadials), and magnetic mineral concentrations/grain size thus have been used as a proxy for determining the strength of ISOW (Kissel et al., 2009; Ballini et al., 2006; Snowball and Moros, 2003).

The spatial distribution in concentration of magnetic minerals and magnetic grain size show coarser grained magnetic minerals near the source in northern Gardar drift and fine-grained magnetic minerals in the southern Gardar drift possibly indicating regional changes in strength of ISOW (Kissel et al., 2009; Ballini et al., 2006). These authors considered single source for magnetic minerals in the Gardar drift i.e., the northern Icelandic basaltic regions. A recent study by Sato et al. (2015) has shown that there are two components of magnetic minerals in the Southern Gardar drift during the late Pliocene-Pleistocene (1) high coercivity component (titanomagnetite) from Icelandic sources brought by ISOW, and (2) low coercivity component (magnetite) from southern sources by NEADW/LDW. They also reported increase in magnetic minerals from Icelandic sources during the early glacial stages of iNHG indicating strengthening of ISOW. While these studies have been carried out on the sediment cores collected at different water depths and during different climatic forcing, a better understanding on provenance of sediments is still needed from the Gardar drift.

Previous studies on the Pb isotopic composition on individual ice-rafted feldspars (>150 μm) from DSDP Site 611 have shown that dominant IRD deposits prior to 2.64 Ma was importantly from the Greenland and Scandinavia, whereas more spread IRD sources (i.e. including NE America) was only after 2.64 Ma (MIS G2) (Bailey et al., 2013). Bailey et al. (2012) further showed changes in the IRD provenance fluxes during the early glacial and full glacial stages at ~2.52 Ma (MIS 100), one of the majors NHG episode, from Archean-aged circum-North Atlantic Ocean continental sources to dominantly Paleozoic and Proterozoic-aged sources, respectively.

3. Materials and methods

3.1. Materials

DSDP Leg 94 Site 611A is located on the southeastern side of Gardar Drift (Baldauf et al., 1987). This Site was drilled at a water depth of 3203.6 m and from the total of 132 m drilled, 99.4 m were recovered (Baldauf et al., 1987). The main goal for drilling this site was to obtain paleoclimate information before, during, and after the intensification of glaciation in the Northern.

The lithology consists of marly nannofossil oozes, foraminiferal - nannofossil oozes with few detrital materials, and marly oozes with more detrital material, alternating with detrital calcareous muds (Baldauf et al., 1987).

A total of 79 samples, corresponding to the 117.15–104.75 m interval (Fig. 2), were collected for investigations. The samples cover the interval between Marine Isotope Stage (MIS) G2 and MIS-99, corresponding to ~2.64 and 2.52 Ma (Bailey et al., 2012).

Age model of DSDP 611A have been performed successfully by Bailey et al., 2013 by linking the benthic $\delta^{18}O$ measured on epifaunal species *C. wuellerstorfi* and infaunal *O. umbonatus* from Bailey et al. (2012) and LR04 (Lisiecki and Raymo, 2007).

3.2. Methods

3.2.1. Physical grain size

The discrete bulk samples were first visually scanned for identifying any coarse lithic fragments. The macroscopic lithic fragments (>1 mm) were found between 112.8 and 113 mbsf. These coarse lithic fragments were separated from bulk samples and their sizes were measured using a scale. The grain size of bulk samples was then analyzed using a Microtrac Bluewave instrument that measures the particle size by laser diffraction in water. All the samples were first treated to remove the organic matter and carbonate content using the 10% hydrogen peroxide (H_2O_2) and 10% hydrochloric (HCl), respectively, for 48 h. The process was repeated twice, and the samples were washed with Milli-Q water after each step. After the complete removal of organic matter and carbonates, sodium pyrophosphate was used to avoid flocculation. For each sample, 1 g of material was placed in laser diffraction equipment for the grain size measurements. The grain size was calculated using the Mie theory for non-spherical particles (Hergert and Wriedt, 2012). Statistical parameters and particle size distribution were analyzed and plotted using the GRADISTAT software version 4 (Blott and Pye, 2001). The analysis was performed at the Centro Oceanográfico de Registros Estratigráficos (CORE), in the Oceanographic Institute of University of São Paulo (IO-USP), Brazil.

3.2.2. Magnetic parameters

The low-field magnetic susceptibility (normalized by volume, κ) was measured directly in 2010 on the u-channels of DSDP Leg 94 Hole 611A at the National Oceanography Centre (NOC), University of Southampton, UK using a Bartington MS2C 100 mm coil, with 1 cm resolution. Further, 64 discrete bulk samples between 117.15 and 104.75 m interval as part of another IODP samples request were analyzed using the Kappabridge MFK1 model at CORE (IO-USP, Brazil).

For particle size specific rock magnetic measurements, all 79 bulk sediments samples were first disaggregated in a 100 ml of 2% sodium hexametaphosphate solution and sieved through a 63 μm mesh, to isolate the sand (>63 μm). The residual material was then separated into following five fractions in settling columns according to the Stokes' law: coarse silt (31–63 μm, 5 ϕ), medium silt (16–31 μm, 6 ϕ), fine silt (8–16 μm, 7 ϕ), very fine silt (4–8 μm, 8 ϕ) and clay (<4 μm, 9 ϕ or more). For each sample, all the six size segregated fractions (sand, coarse silt, medium silt fine silt, very fine silt and clay) were analyzed for rock magnetic parameters.

To understand the magnetic concentrations, and magnetic grain size variations using the Day Plot, hysteresis loop and backfield isothermal remanent magnetization (BIRM) was measured for all the six distinct size fractions of 79 bulk samples (total 474 sample size) using a Vibrating Sample Magnetometer (VSM) MicroMag 3900 Princeton Lake Shore Cryotronics at CORE (IO-USP, Brazil). A maximum field of 1 T was applied for measuring the hysteresis cycle, with most samples saturating well below 500 mT. The hysteresis results were processed using the HystLab software (Paterson et al., 2018), and parameters saturation magnetization (Ms), saturation remanence (Mrs), and coercive force (Hc) were calculated from slope (paramagnetic) corrected hysteresis cycle. BIRM was used to obtain the coercivity of remanence (Hcr).

Thirteen representative samples of different size fractions of glacial and interglacial intervals were analyzed for the first-order reversal curves (FORCs) to characterize the magnetic domains. Additionally, six coarse lithic fragments (IRD) found between 112.8 and 113 mbsf were also analyzed for FORC measurements. The 270 FORCs were measured for each sample with an averaging time of 0.5 s and 0.1 s of slew rate between successive measurements. The FORC diagrams were processed using Forcinel 3.0 software enabled with Variforc function (Harrison and Feinberg, 2008; Egli, 2013). The smoothing factors of Sc0 = 7, Sc1 = 7, Sb1 = 7, and Sb0 = 3, horizontal and vertical lamda of 0.1, and output grid of 1 were used.

Temperature dependence of magnetic susceptibility (χ-T) on

representative samples of different size fractions from glacial and interglacial interval was also measured up to a maximum temperature of 700 °C in an argon atmosphere using a furnace-equipped KLY-4 AGICO Kappabridge instrument to constrain the magnetic mineralogy.

4. Results

4.1. Grain size

A total of 38 macroscopic lithic fragments of >1 mm, identified as IRDs, were found in three levels at 112.8 mbsf (10 pcs.), 112.9 mbsf (20 pcs.), and 113 mbsf (8 pcs.), respectively (Fig. 2). The largest lithic IRD fragment has a diameter of 1.5 cm and was found at 112.9 mbsf. The microscopic observation of these lithic fragments showed granites, basalts, gabbro, gneiss, quartzite and sandstone composition. The coarse lithic frgaments (2 mm and 250 μm) are related to the dynamic of the calving margins and can be termed as iceberg rafted debris (IBRD) (Krissek, 1995; Wilson et al., 2018). Of these 38 macroscopic lithic fragments, several coarse lithics were identified as IBRD.

The lithology of the bulk sample is represented by mud and characterized by very poor sorting, with symmetrical curve and platykurtic. The mean grain size of studied interval is 0.725 μm, with a standard deviation of 0.038 μm. The largest particle size was 1.7 μm at 108.95 mbsf, and smallest particle size was 0.256 μm at 108.75 mbsf. Overall, the clay varies between 51.6 and 83.6% (average = 64.6%), and silt fraction varies between 14.1 and 40.8% (average = 31.8%) (Table 1). The sand shows minimum concentration and varies between 0 and 13.5% (average = 3.6%) (Table 1). The silt fraction was further subdivided into four subclasses i.e., coarse silt, medium silt, fine silt and very fine silt and their relative distribution is given in Table 1.

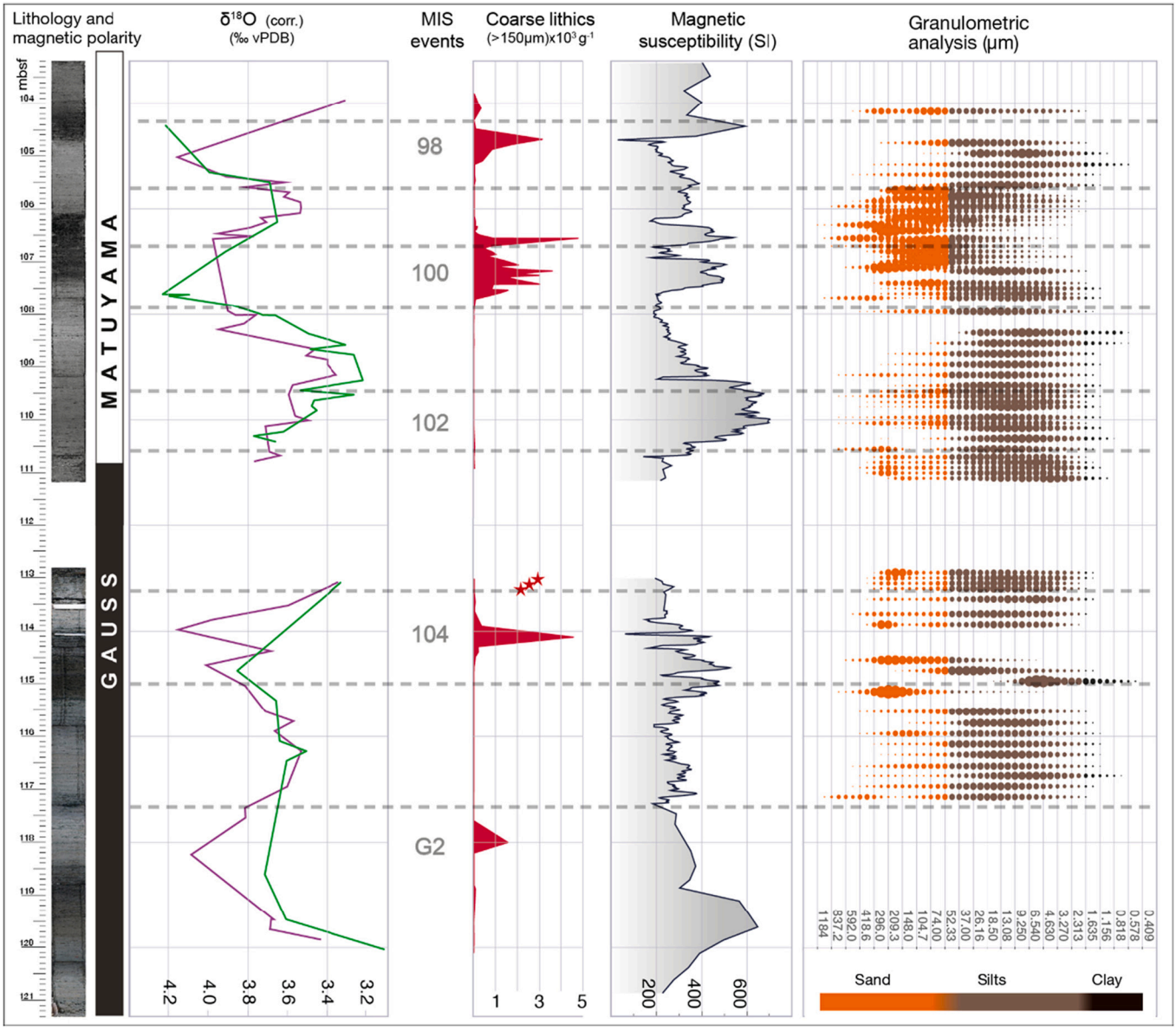

Fig. 2. Benthic $\delta^{18}O$ measured on epifaunal species *C. wuellerstorfi* (adjusted by adding 0.64%, purple line) and infaunal *O. umbonatus* (green line) from Bailey et al., 2012, IRD abundance (Bailey et al., 2013), magnetic susceptibility measured on u-channels and sediment particle size variations from the studied interval. Particle size variation can be easily observed in the core. Larger circle symbols represent a higher percentage of grains of the specific grain size, while smaller circles represent a lower percentage of particles of that specific grain size. Note that less intense glacial intervals (MIS 102) when compared to MIS 100 or MIS 104, contain little or no IRD material. In the grain size plot, it is possible to observe that a major part of grains is clay and silt. The red starts are a level with Iceberg Rafted Debris (IBRD) very larger, >0.5 cm. (For interpretation of the references to colour in this figure legend, the reader is referred to the web version of this article.)

Table 1
Composition of different grain size fractions of studied interval.

	Sand (%) (>63 μm)	Coarse Silt (%) (63–31 μm)	Medium Silt (%) (16–31 μm)	Fine Silt (%) (8–16 μm)	V. Fine Silt (%) (4–8 μm)	Clay (%) (<4 μm)
Average	3.6%	3.4%	5.0%	6.7%	8%	73.3%
Minimum	0.0%	0.0%	0.0%	0.9%	6.1%	58.7%
Maximum	13.5%	6.9%	7.5%	8%	8.7%	91.3%

The grain size data was plotted with depth, stable isotopes, magnetic susceptibility and is presented in Fig. 2. The sand shows opposite behavior to clay and silt distribution (Fig. 2). The sand shows minimum concentration during most of the interglacial periods e.g., MIS G1, 101 and 103, whereas medium silt and clay fraction dominated the overall sediment assemblages during these intervals (Fig. 2). The high percentage of sand and coarse silt was found between ~107.7 and 106.3 mbsf (MIS 100 and 99) (Fig. 2). During the MIS 100 glacial period, fine silt and clay concentration has reached minimum, whereas during the end of MIS 99 interglacial interval clay and silt fraction has again increased significantly (Fig. 2).

4.2. Magnetic parameters

4.2.1. Magnetic susceptibility

The u-channel magnetic susceptibility (κ) results show highly variable distribution in concentration of magnetic minerals during the studied interval (Fig. 2). κ varies from 700 10^{-6} SI at 110 and 119 mbsf to 100 10^{-6} SI at 105 mbsf (Fig. 2). The κ shows a relatively higher concentration during the glacial periods MIS 104, 102 and 100, whereas intermittent interglacial periods MIS G1 and 101 show a decline in susceptibility values (Fig. 2). Bailey et al. (2012) identified at least six IRD events during the MIS 100 glacial as shown by coarse lithic data (Fig. 2). During these MIS 100 IRD peak episodes, the κ also shows peaks in values, mimicking the coarse lithic data (Fig. 2). Interestingly, during the MIS 99 interglacial, the κ has also increased and covaries with sand and coarse-silt abundance.

4.2.2. Thermomagnetic curves

Thermomagnetic curves (Fig. 4) show presence of magnetite in all the studied different size fractions of glacial and interglacial period sediments. Hematite was also found in few samples e.g., 115.95 m (fine silt) and 116.95 m (medium silt). The thermomagnetic curves of most samples are almost or completely reversible (106.15 (sand), 106.4 (very fine silt), 106.5 m (coarse silt), 115.95 m (fine silt) and 116.95 m (medium silt)).

4.2.3. Hysteresis loops and Day plot

The particle-size specific results on various hysteresis and BIRM parameters (Ms, Mrs, Hc and Hcr) and their ratios (Mrs/Ms and Hcr/Hc) are provided in Supplementary Tables 1 and 2. A stack of hysteresis loops of different particle sizes shows two distinguishable signatures "A and B" (Fig. 3). The signature "A" shows saturation well below 500 mT and have relatively wide central part of the hysteresis loop compared to the signature "B" that has relatively more constricted central part, signifying the differences in coercivities distribution of two signatures. Further, few samples carrying "B" signature of hysteresis loop,don't acquire saturation in 500 mT applied field and indicates mixed low and high coercivities minerals/grain size than "A" signature. The "B"

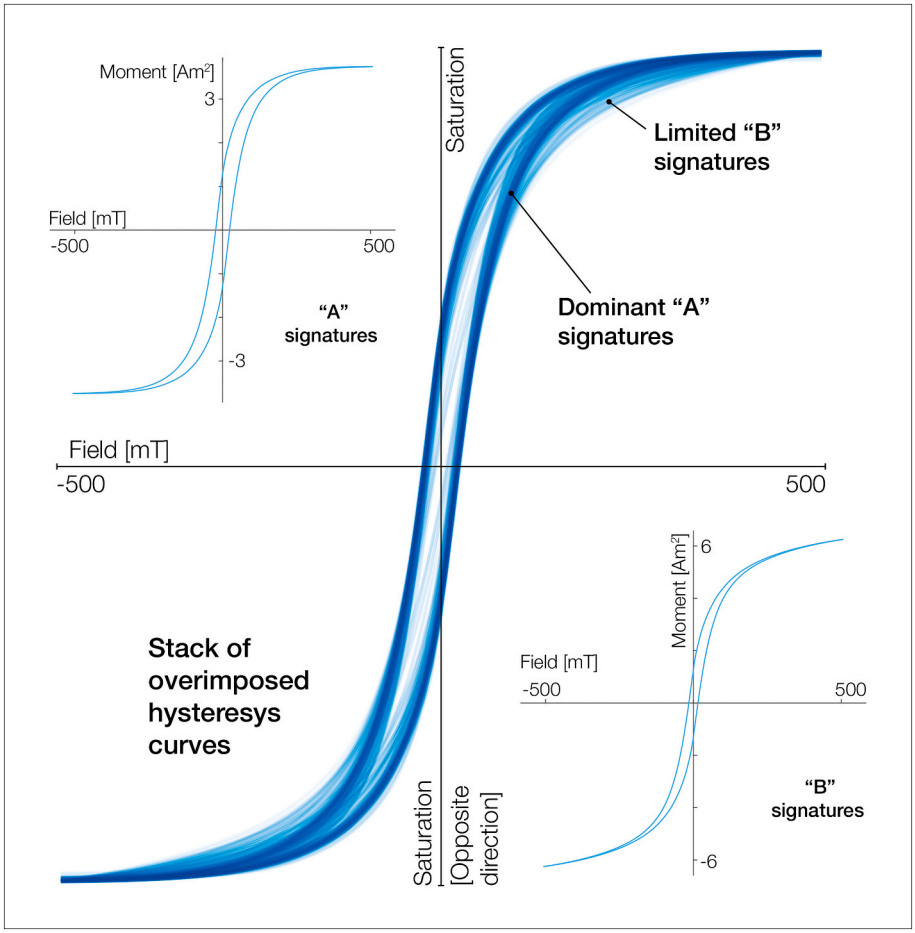

Fig. 3. Stack of all hysteresis loops of various size fractions. Note that the vertical axis represents the magnetic moment. The stack shows a very consistent "A" signature (see medallion), marked by the darker blue overlap in the stack. Few samples diverge from this signature due to the presence of a secondary "B" signature in the mix. Here, we showed with 500 mT field just for better view of hysteresis loops forms. (For interpretation of the references to colour in this figure legend, the reader is referred to the web version of this article.)

signature shows a persistent paramagnetic signal. The signature "A" is shown by large number of samples (~85%).

For the Ms and Mrs, normalized by mass, the higher average values correspond to fine silt, followed by coarse, medium, and very fine silt, while sand and clay fractions show lower values Supplementary Table 1 and Fig. 5. The maximum values of Mrs/Ms are shown by very fine silt and minimum by sand, whereas different silt fractions and clay show similar mean Mrs/Ms values (Fig. 5) Hc and Hcr values are minimum for sand and maximum for the very fine silt fraction Supplementary Table 2 and Fig. 5. The Hcr/Hc ratio is higher in the sand, followed by coarse silt, clay, and fine silt.

The Day plot for different particle size fractions during the glacial and interglacial intervals is shown Fig. 9 (Day et al., 1977; Dunlop, 2002). The different particle size fractions of sediments fall in the pseudo-single domain (PSD) region of the Day plot and are closely associated. The sand size fractions of glacial interval sediments show relatively higher diversity in the Day Plot (Fig. 9), with several samples showing coarser PSD range.

4.2.4. FORCs

The FORCs results on different sediment fractions of interglacial and glacial intervals, and on coarse IBRD lithic fragments >0.5 cm and < 1.5 cm are presented in Figs. 6 and 7, respectively. We chose the most representative samples, with the highest and lowest Mrs/Ms ratio, for different granulometric fractions.

Overall FORC diagrams of the sediment samples show the presence of interacting single domain (SD) low coercive (between 60 and 80 mT) ferrimagnetic particles (Fig. 6). Coercivity range and magnetostatic interaction for the different size fractions i.e., coarse silt, fine silt, and clay fractions of both glacial and interglacial intervals remain constant. While sand fraction from interglacial interval also did not show any distinguishable feature from the rest of particle size fraction's FORC, sand fraction from glacial interval recovered at 106.21 mbsf show distinct behavior with relatively lower coercivity (Hc ~40 mT) and higher vertical interaction (Hu >40 mT) indicating PSD to the MD ferrimagnetic component (Fig. 6). The FORC diagrams further corroborate with the results of Day Plot showing that there is only little

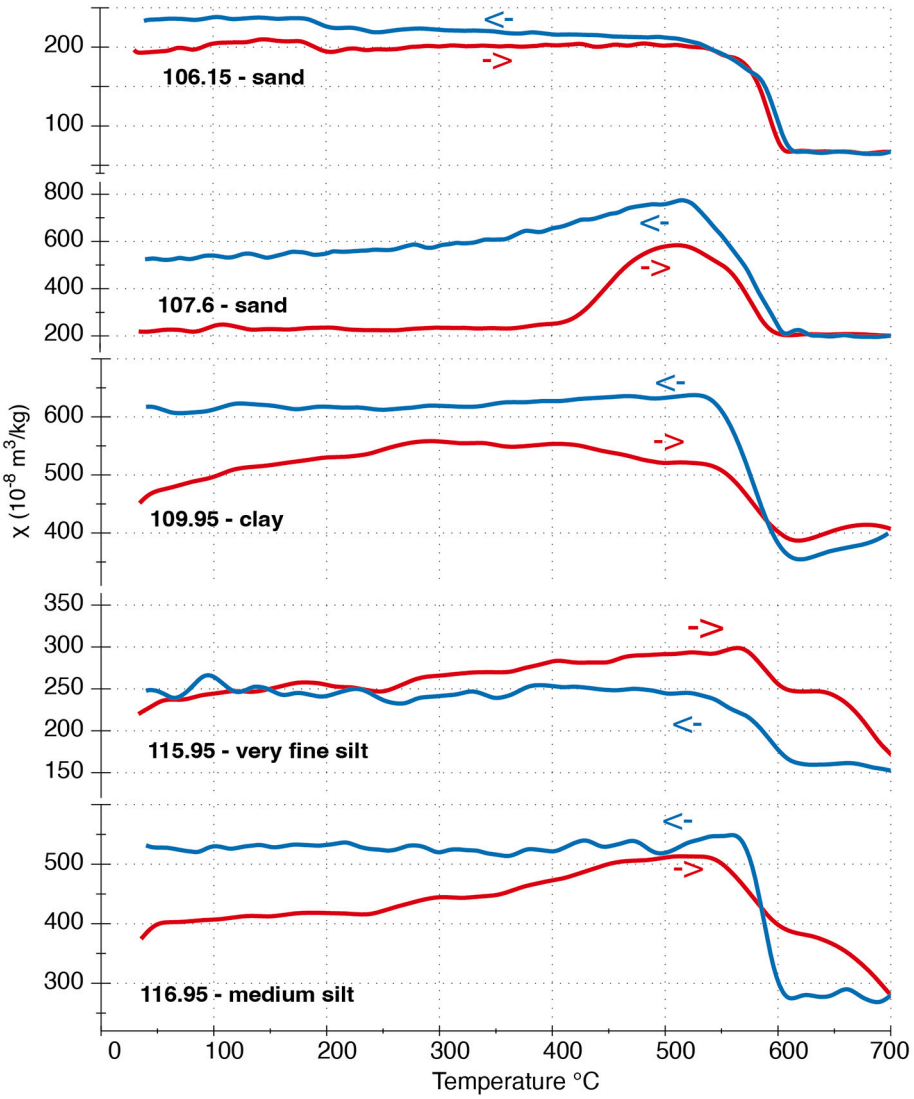

Fig. 4. Temperature-dependent magnetic susceptibility curves of seven selected samples. All samples present the Curie point of magnetite at 580 °C, making it possible to use the Day Plot in these analyses.

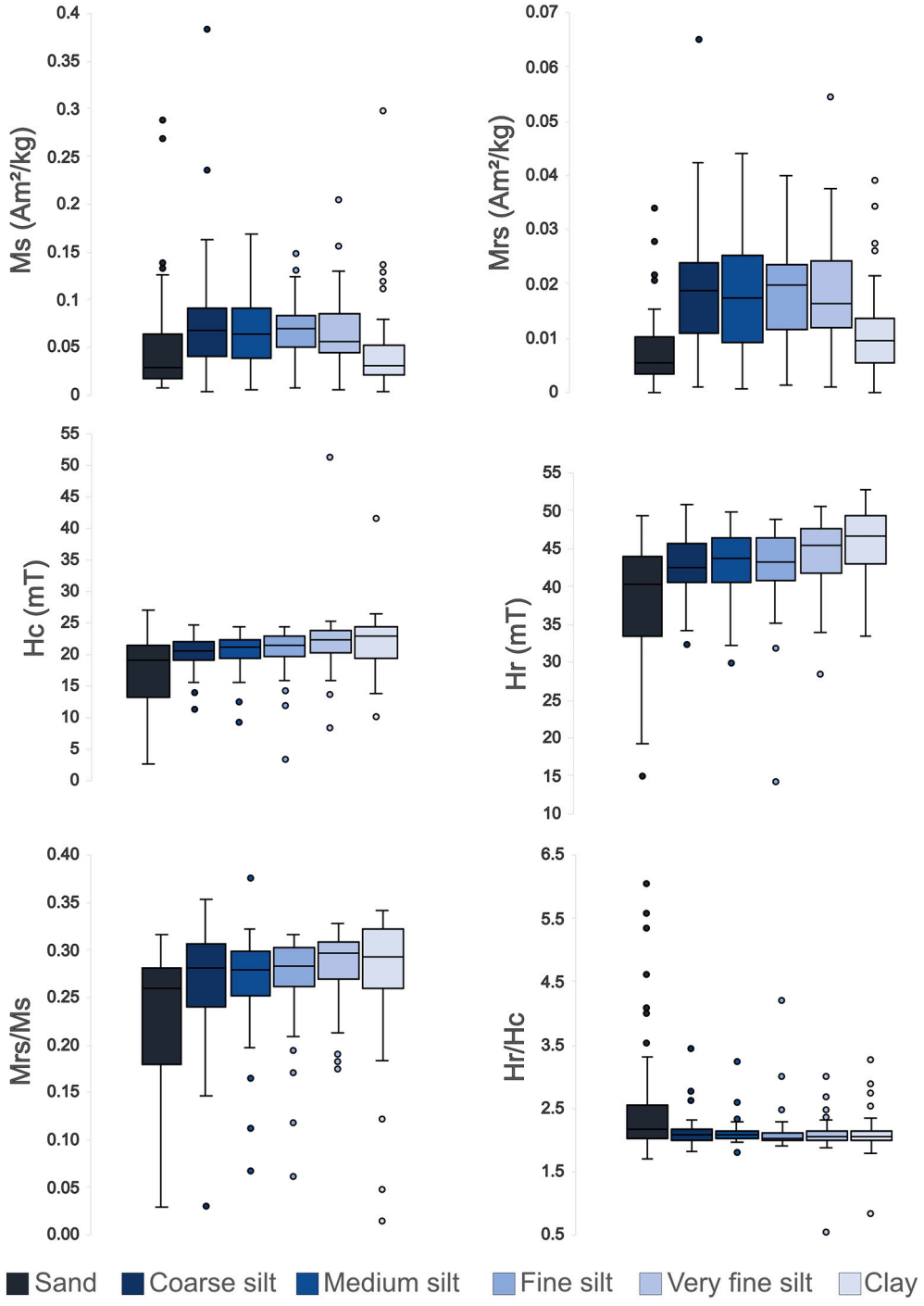

Fig. 5. Graphs of the distribution of Ms, Mrs, Hc, Hcr, Mrs/Ms and Hcr/Hc values in the six particle size fractions studied.

variation between the finer particle size fractions (silt and clay).

FORCs of coarse lithic IBRD exhibit a variety of signals (Fig. 7). Basaltic samples represent the majority of IBRD. These basalts show SD to PSD particles with the Hc values lower than 30 mT while the Hu values approach 50 mT. However, one basaltic sample, hereby identified as altered basalt, shows SD particle with a very strong negative interaction of up to 120 mT on the Hc axis, while the Hu axis ranges from a few mT to 10mT (Fig. 7). IBRD characterized as granodiorites reveal low coercive multi-domain particles with the Hu values ranging from 10 mT to 100 mT while the Hc values are between 40 and 60 mT (Fig. 7). Alkali feldspar granite is the only IBRD sample that shows no magnetic signals. One sample identified as gabbro shows Hc values between 40

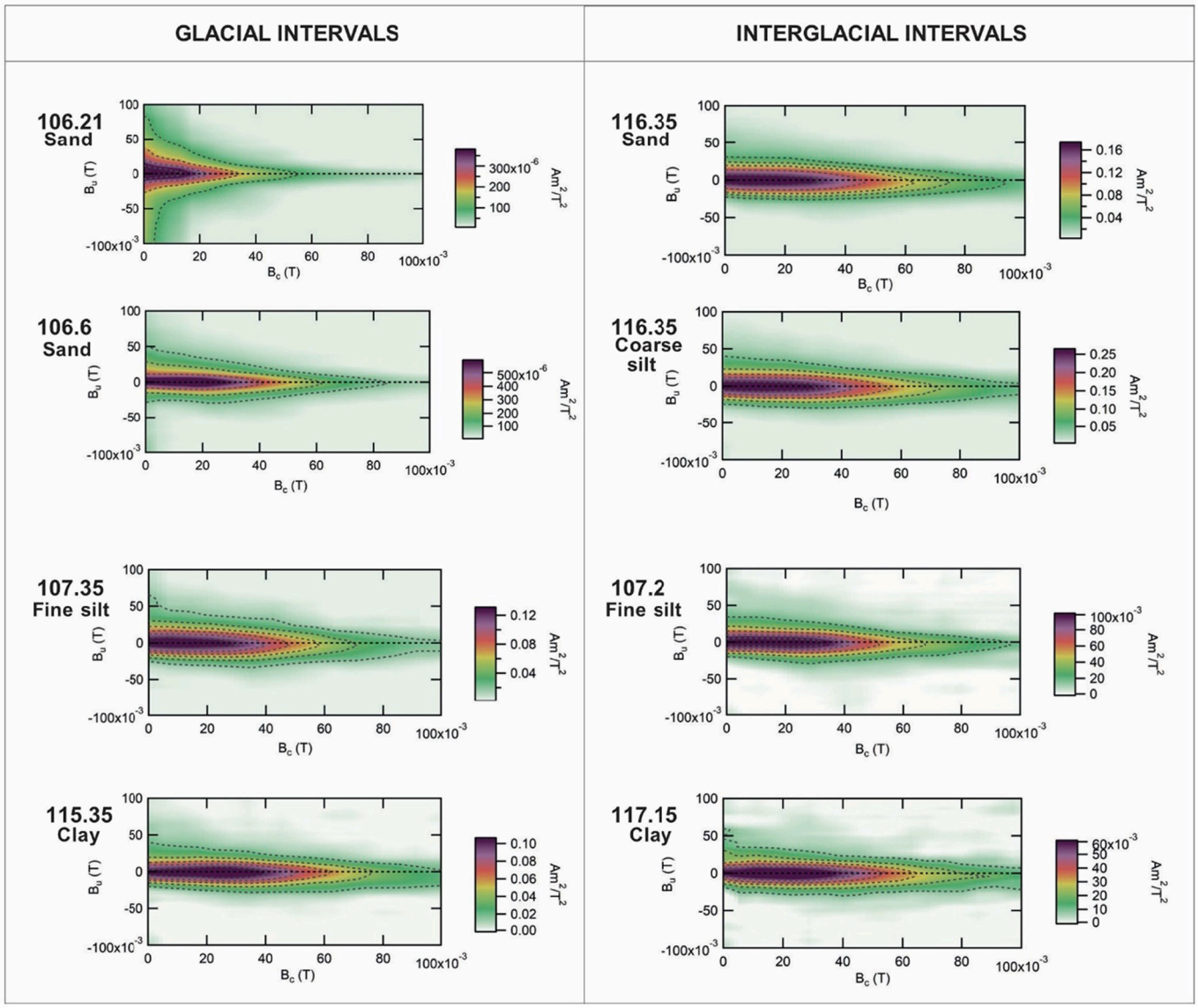

Fig. 6. FORCs of selected sand, coarse silt, fine silt, and clay for samples from glacial and interglacial intervals.

and 80 mT and Hu values go up to 60 mT. Gneiss contains multi-domain magnetic particles with coercivity spectra of up to 70 mT. The sample identified as sandstone contains low coercivity SD-magnetic particles (Fig. 7).

5. Discussion

5.1. Magnetic grain size as proxy for provenance

This work used a new and unusual methodology to establish the sediment provenance during the glacial and interglacial intervals of the early Pleistocene. Different geochemical proxies are used to study provenance; however, these proxies are usually destructive, expensive, and require a greater amount of sample mass.

This study shows that the use of magnetic parameters can be applied to provenance studies effectively avoiding the disadvantages from other methods. For all magnetic analyses used in this work, we used <1 g of sample of each magnetic fraction. Only the magnetic susceptibility analysis with temperature dependence was destructive, and it was applied to a limited number of samples weighing <0.35 g.

One of the objectives of separating the different magnetic fractions from the silt fraction was to verify if there was a difference in the results of these fractions among themselves and with the clay fraction. This is the most time-consuming part of the analysis, as according to Stokes' Law, pipetting is required. It was found that all the silt fractions and the clay fraction have very similar results to each other, with only the sand fraction showing diverging results. Thus, it is possible to make the preparation for these analyses even faster, with only the separation of the clasts and sand fraction from the rest of the material, or at most the separation of the silt and clay fraction. However, it is necessary that sand is always separated from the silt and clay fraction, since particles of these different sizes have different hydrodynamic behavior, reflecting

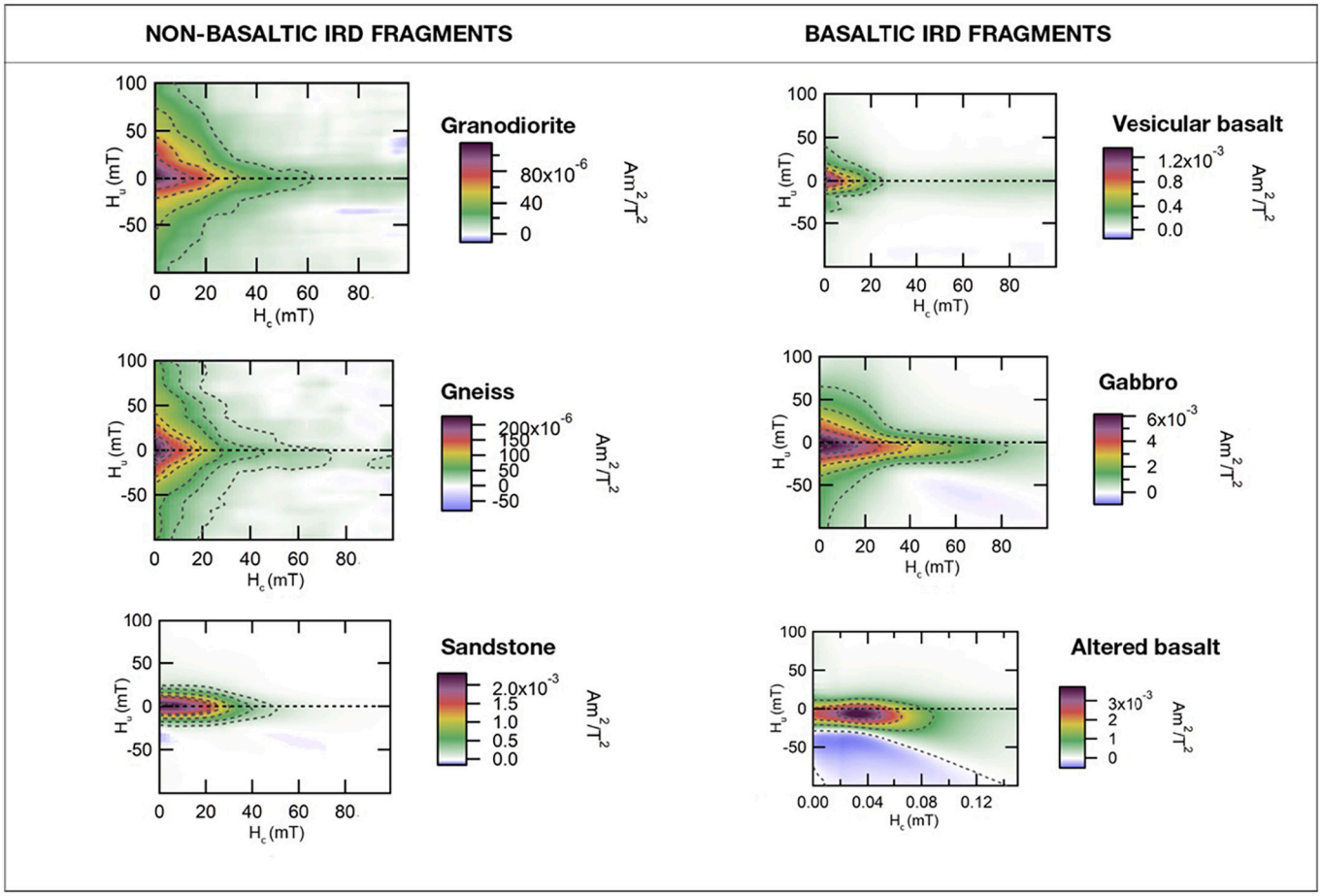

Fig. 7. FORCs of selected IBRDs, characterized by basaltic and non-basaltic signatures. Non-basaltic IRDs include granodiorite, gneiss, and sandstone while the basaltic IRDs include vesicular basalt, gabbro and altered basalt.

very different aspects of environmental responses, especially in glacio-marine environments, since particles of the sand fraction are usually IRD.

By optimizing sample preparation, it is possible to perform provenance studies using magnetic parameters at a higher resolution.

Another consideration for using magnetic method is that the possible source areas must be known. The magnetic parameters for the study area must be accomplished to perform the characterization unless these values are already available in the literature. The magnetic properties of the source areas should differ significantly, primarily in the magnetic grain size to physical grain size ratio.

5.2. *Characterizing sediment sources in the Gardar Drift*

The subpolar North Atlantic sediments have been a subject of detailed investigation for characterizing the sediment provenance to understand the oceanic circulation and extent of ice-shelf glaciation in the Northern Hemisphere. Bailey et al. (2012, 2013) studied the Pb isotopic signatures from coarse lithic Feldspars recovered from the Gardar drift DSDP Site 611 for the late Pliocene-Pleistocene interval and suggested that Greenland and Scandinavia were the dominant source of the IRD in the subpolar North Atlantic prior to the MIS G2 glacial period, whereas IRD contributions from the North America has increased afterwards. In the current study, we found an additional level of the coarse macroscopic lithic (IBRD) rock fragments between 112.8 and 113 mbsf, corresponding to the glacial-interglacial transition interval of MIS 104 to MIS 103 (Fig. 2). These rock fragments showed varied compositions e.g., basalts, granites, granodiorites, sandstones. FORCs result on these coarse lithic rock fragments, showed distinguished characteristics (SD-MD magnetic particle) compared to the bulk sediments that show mainly PSD magnetic particles (Fig. 7). The coarse lithic rock fragments are composed not only of basalts but also of granites and granodiorites compositions. Therefore, these coarse lithics at this interval could have been supplied by wind-driven surface currents discharging Icebergs brought materials from Iceland-Greenland as well as from the North America that have such rock compositions. While our observations regarding the coarse lithic rock fragments are limited to microscopic observations and FORC measurements, Bailey et al. (2013) had provided more concrete evidence based on the Pb isotopic compositions of coarse lithic Feldspar during the MIS 104 from the DSDP 611 and had suggested similar provenances of IRD.

Previous studies on geochemical and magnetic properties of terrigenous fractions of the Gardar drift have suggested two distinguishable compositions; (1) titanium rich mafic basaltic fractions, and (2) relatively acidic (/felsic) sediments rich in potassium (here referred as non-basaltic) (e.g., Kissel et al., 2009; Ballini et al., 2006; Gruetzner and Higgins, 2010). The different composition of terrigenous fractions shows a great dependency on glacial-interglacial climatic variability. The higher basaltic fractions are brought by southward flowing deep-water ISOW during interglacial from the Iceland and the Faeroe Islands (Kissel et al., 2009; Ballini et al., 2006; Hayashi and Ohno, 2021), whereas non-basaltic felsic sediments are sourced from the surrounding continental rocks brought either by Icebergs (Ballini et al., 2006) and/or by NEADW/LDW when ISOW had shoaled during glacial (Gruetzner and Higgins, 2010). Sato et al. (2015) and Hayashi and Ohno (2021) were able to distinguish two magnetic components (1) high coercivity

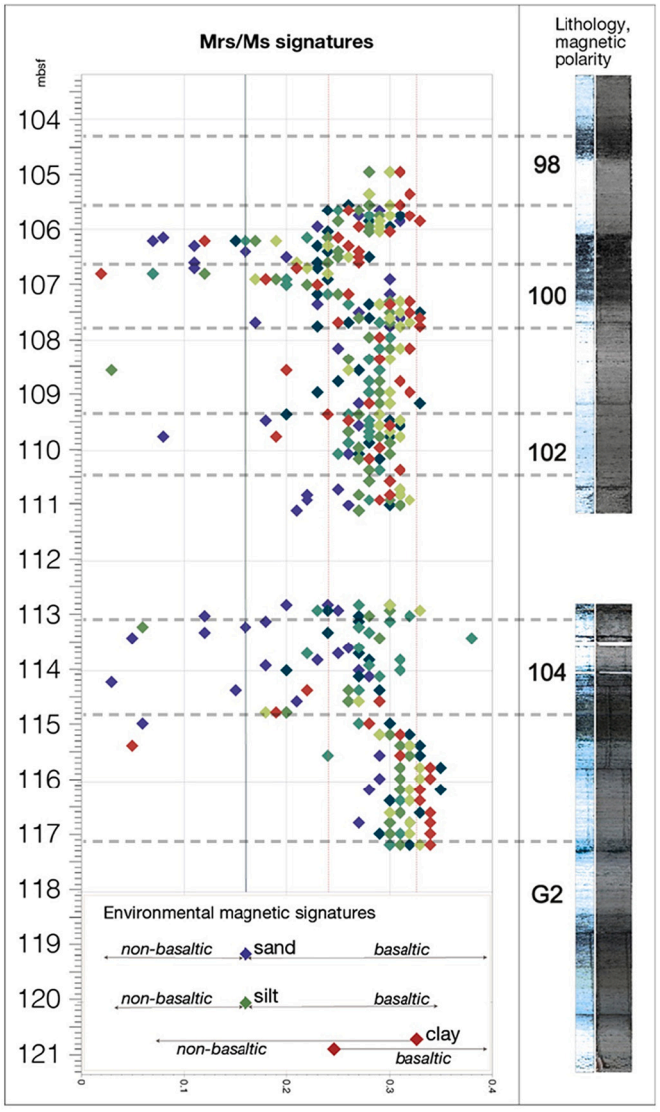

Fig. 8. Mrs/Ms ratios (middle) and basaltic/non-basaltic signatures derived from the interpretation of the magnetic results (right).

component (titanomagnetite) from Icelandic sources brought by ISOW, and (2) low coercivity component (magnetite) from southern sources by NEADW/LDW in the Southern Gardar drift.

In this work, we use particle-size specific magnetic properties (Mrs/Ms) to distinguish different provenances of the Gardar drift sediments. Hatfield et al. (2013 and 2017) studied particle-size specific magnetic properties of glacial-fluvial sediments collected near the Greenland and Iceland margins and attributed Mrs/Ms ratios with a mean of 0.26 and range from 0.16 to 0.36 for the basaltic sediments of Iceland. They attributed Mrs/Ms ratio from 0.24 to 0.49 for clay; 0.16–0.35 for silt and0.16–0.40 for sand. Greenland sediments (non-basaltic provenance) have a Mrs/Ms ratio with a mean of 0.06 and ranges between 0.02 and 0.15 (Hatfield et al., 2017). Hatfield et al. (2017) attributes Mrs/Ms ratio ranges from 0.07–0.33 for clays; 0.03–0.15 for silt; 0.02–0.14 for sand of Greenland sediments. We use these subdivisions to distinguish the Icelandic and Faroe Island basaltic sediments and Greenland (non-basaltic sediments) for clay and sand fractions. For subdivisions of silt fractions like coarse, medium, and fine silt, we use the magnetic characteristics of the modern sediments available for the Norwegian-Greenland Seas in Hatfield et al. (2019). Further, Mrs/Ms of most of the coarse, medium, fine and very fine silt fractions fall within Mrs/Ms range of Icelandic silt. Some clay fractions were not directly classified, because they have an overlap between the magnetic grain size of basaltic and non-basaltic clay. However, it is possible to conclude that the dominant fraction is basaltic. The hydrodynamic behavior of clay and silt size fractions is very similar (McCave et al., 1995). Based on this comparison, we were able to distinguish the provenance of different size-fractions which is shown in Fig. 10. The different size fractions (i.e., sand, silt and clays) of most of the samples of both glacial and interglacial interval show basaltic signatures, falling within fine PSD range (Figs. 8 and 9). The magnetic grains sizes of Icelandic basaltic samples do not show any dependency on physical grain sizes and show homogeneity (Hatfield et al., 2013). This is further supported by the FORC measurements on different size fractions of glacial and interglacial interval showing similar signature (Fig. 6). Hatfield et al. (2013) have shown that only fine silt and clay fraction of Greenland are as fine as Icelandic sediments, whereas coarse silt and sand show distinguished magnetic grain sizes falling in the coarse PSD and MD zone. Coarse silt and sand of non-basaltic magnetic signature is associated to IRD. In the studied interval, only sand fractions of few samples (13 samples) of the Glacial MIS 104 and 100 clearly showed non-basaltic signatures (Fig. 8). This is further supported by independent observations made by Hassold et al. (2006), who suggested that silt and clay fractions in the Gardar drift are from Iceland and are brought by ISOW. The MIS 104 and 100 are intense glacial events, as observed in oxygen isotopic data (Lisiecki and Raymo, 2007), and therefore likely brought more IRD deposits from Greenland, Scandinavia, and North America. Consequently, more sand-sized particles are transported in this region during MIS 104 and MIS 100 glacial events and is recorded by magnetic grain size data. While MIS 102 is relatively less intense glacial event, and thus non-basaltic sands are absent. However, our study is limited by non-availability of particle-size specific magnetic data from other IRD and IBRD probable provenances like North America. Overall, particle size specific measurements of magnetic parameters can indicate different provenances and glacial-interglacial strengths.

5.2.1. *Characterization of glacial intervals*

The analysis of sediment particle size provides new information on sediment supply during glacial-interglacial cycles. These analyses allow us to observe varying behaviors in different glacial and interglacial intervals. Glacial intervals have three distinct characteristics: a coarser average particle size, a higher average percentage of sand, and a higher number of non-basaltic particles, primarily in the sand fraction. These characteristics, however, are distinct in each glacial interval.

MIS 104 has the second highest input of predominantly non-basaltic particles, primarily from the sand fraction, and is the only level with IBRD larger than 0.5 cm; however, the average particle size (0.633 μm) is like the average size of MIS G1 particles but larger than other interglacial and glacial periods, such as MIS 103, MIS 102, and MIS 101 with the average 2.8% percent sand. We have identified new levles containing IRD clasts (>150 μm), located above the level with IRD described by Bailey et al. (2013). The IRD clasts discovered in this study, dating from the end MIS 104 - beginning of MIS 103, are most likely associated with the deglaciation. MIS 102, on the other hand, has essentially interglacial characteristics, which can be attributed to IBRD with the average particle size (0.542 μm), the average percentage of sand (1.7%), or the low presence of non-basaltic particles. In comparison to interglacial periods, the amount of IRD (larger than 150 μm) revealed by Bailey et al. (2013) is also close to zero.

During full glacial and late glacial conditions, MIS 100 has the highest mean sand value (6.5%), the largest mean particle size (1.048 μm), or the highest input of non-basalt particles, primarily in the sand fraction. The highest amount of IRD was also found by Bailey et al. (2013) of all glaciers studied, with several peaks throughout the interval, the largest being near the transition with MIS 99.

This allows different glacial MIS to be distinguished. As previously stated, MIS 102 is regarded as a less intense glacial interval, more akin to interglacial intervals. Glacial intervals 100 and 104 are regarded as

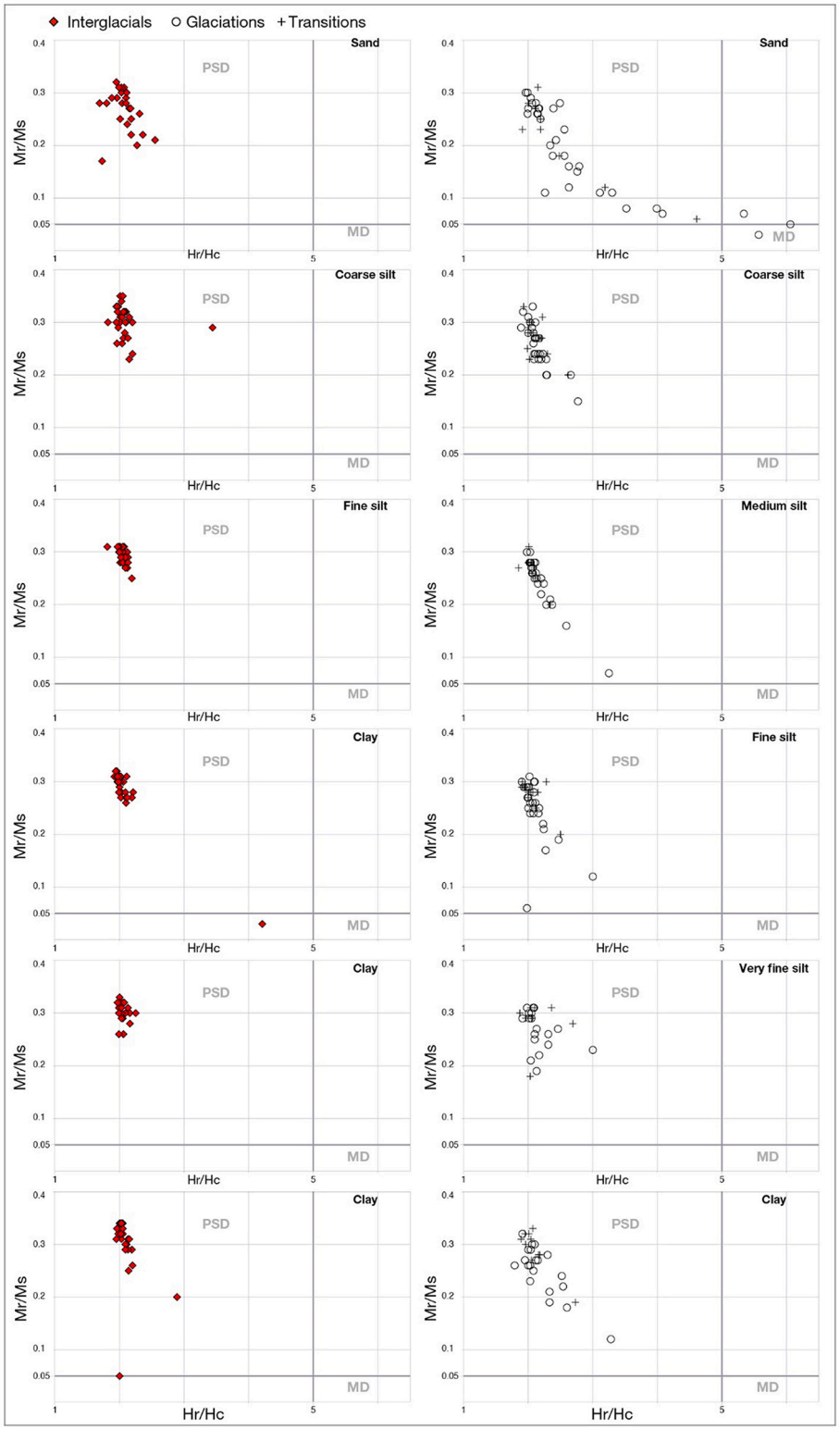

Fig. 9. Day Plot of sand, coarse silt, fine silt, and clay fractions. In the plot, it is possible to see that most of the samples are in the pseudo-single domain, with few samples in the multidomain, mainly the sand fraction. The left side of figure shows interglacial samples. The transitions of interglacial/glacial or glacial/interglacial and glacial periods are in the right side.

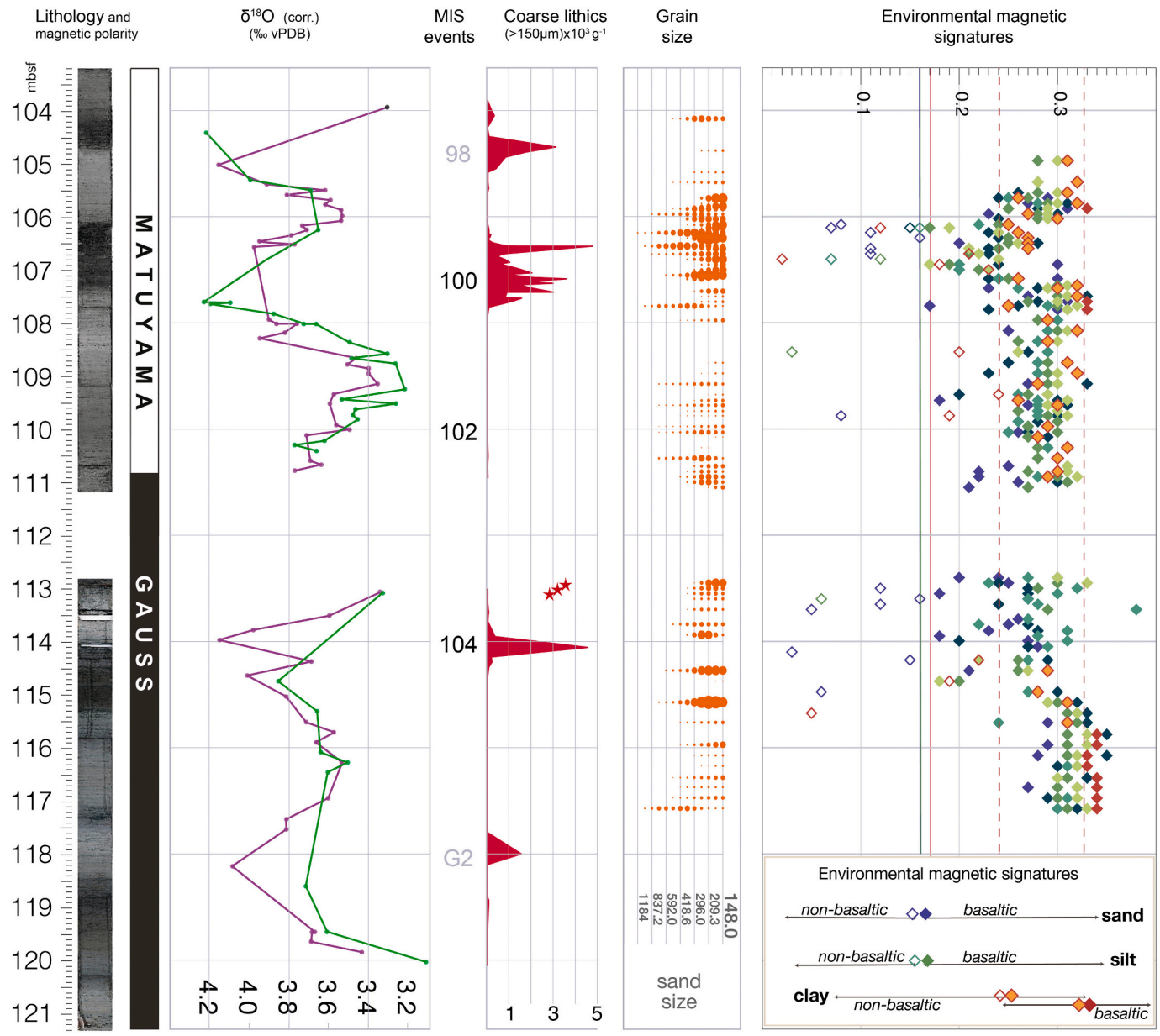

Fig. 10. Provenance signatures identified by grain size analysis and environmental magnetism compared with benthic $\delta^{18}O$ measured on epifaunal species *C. wuellerstorfi* (adjusted by adding þ0.64‰, purple line) and infaunal *O. umbonatus* (green line) from Bailey et al., 2013, IRD counts,magnetic susceptibility and environmental magnetic signatures. A background basaltic signature (probably detrital) is present in all samples. The blue and red shaded bars marked the non-basaltic signatures (red) and basaltic signatures (blue). During glacial interval signatures vary, either dominated by basaltic or by non-basaltic signatures. Note the non-basaltic provenance is dominant or significant after the glacial peaks in the case of strong glaciations (MIS 100 and MIS 104). The weaker glaciation at MIS102 is characterized by weak/absent non-basaltic signatures. Non-basaltic signatures appear occasionally also in interglacial levels. (For interpretation of the references to colour in this figure legend, the reader is referred to the web version of this article.)

intense glacial intervals in the literature (Raymo et al., 1989). It is possible to observe, even though these two intervals were intense glacial periods, MIS 100 is even more intense than MIS 104. In the transition to interglacial MIS 99, glacial intervals as intense as MIS 100 continue to have input from larger, non-basaltic particles. This deposition occurs in already deglacial conditions.

6. Conclusions

In this work, we studied physical grain size and magnetic grain size parameters of MIS 104 to MIS 99 of DSDP Leg 94 Hole 611A. From a methodological point of view, the relation between magnetic grain size and physical grain size makes it possible to differentiate a sediment source area, in a faster, non-destructive, and less expensive way than compared to other geochemical techniques. When the magnetic grain size is compared to the physical grain size, it is reasonable to conclude that the large percentage of the granulometric fractions of the analyzed samples are basalt-rich Icelandic sediments. These grains are classified as fine PSD, and are consistent throughout the analyzed core.

Grain size fractions of some samples considered non-basaltic are sand that occur during more intense glacial periods (MIS 100 and 104) and transitions from these glacial to interglacial periods. These particles are mostly coarse PSD. Because of the increase in grain size during glacial intervals, particularly during the transition to glacial intervals, these non-basaltic grains can be classified as IRD. As the studied region is separated from the landmass by icebergs, IBRD from Greenland or other

non-basaltic sources such as North America are also a significant source of IRD for the region.

The glacial periods could be distinguished by three distinct characteristics: larger average particle size, a higher average percentage of sand, and a higher presence of non-basaltic particle, particularly in the sand fraction. Each glacial period, however, has its signature. Because of the higher percentage of sand, larger average particle size, and greater presence of non-basaltic granulometric fractions, MIS 100 can be considered the most intense during the study period, while MIS 104 exhibits similar but less pronounced characteristics.

Author contributions statement

SL, DP, and LJ designed and developed the study; SL performed the grain-size measurements; SL and MBH performed the rock-magnetic experiments; SL, LJ, DP, PS and JRM interpreted the results; DP, PS, JRM and SL developed the concepts; all authors participated at the writing of the manuscript.

Data and materials availability

All data are available in the main text or supplementary materials.

Funding

DP acknowledges the Fundação de Amparo à Pesquisa do Estado de São Paulo (FAPESP) for financial support through grant 2018/20733-6. PS acknowledges FAPESP Postdoctoral grant 2019/11364-0. MBH acknowledges FAPESP grant # 2017/04821-0. This publication is also part of DP's project "Impact of sea-level rise on anoxic basins: Paratethys vs. Black Sea" (project number VI.Veni.212.136), of the research programme VENI which is financed by the Dutch Research Council (NWO). LJ acknowledgment of funding of FAPESP project 2016/24946-9.

Declaration of Competing Interest

The authors declare no competing interests.

Data availability

Data will be made available on request.

Appendix A. Supplementary data

Supplementary data to this article can be found online at https://doi.org/10.1016/j.gloplacha.2022.104022.

References

Baldauf, J.G., Thomas, E., Clement, B., Takayama, T., Weaver, P.P., Backman, J., Jenkins, G., Mudie, P.J., Westberg-Smith, M.J., 1987. Magnetostratigraphic and biostratigraphic synthesis, Deep Sea Drilling Project Leg 94. Initial Reports of the Deep Sea Drilling Project 94 (part 2), 1–59.

Bailey, I., Foster, G.L., Wilson, P.A., Jovane, L., Storey, C.D., Trueman, C.N., Becker, J., 2012. Flux and provenance of ice-rafted debris in the earliest Pleistocene sub-polar North Atlantic Ccean comparable to the last glacial maximum. Earth Planet. Sci. Lett. 341, 222–233.

Bailey, I., Hole, G.M., Foster, G.L., Wilson, P.A., Storey, C.D., Trueman, C.N., Raymo, M. E., 2013. An alternative suggestion for the Pliocene onset of major Northern Hemisphere glaciation based on the geochemical provenance of North Atlantic Ocean ice-rafted debris. Quat. Sci. Rev. 75, 181–194.

Ballini, M., Kissel, C., Colin, C., Richter, T., 2006. Deep-water mass source and dynamic associated with rapid climatic variations during the last glacial stage in the North Atlantic: a multiproxy investigation of the detrital fraction of deep-sea sediments. Geochem. Geophys. Geosyst. 7.

Bianchi, G., McCave, I., 2000. Hydrography and sedimentation under the deep western boundary current on Bjorn and Gardar drifts, Iceland Basin. Mar. Geol. 165 (1–4), 137–169.

Blake-Mizen, K., Hatfield, R.G., Stoner, J.S., Carlson, A.E., Xuan, C., Walczak, M., Lawrence, K.T., Channell, J.E., Bailey, I., 2019. Southern Greenland glaciation and western boundary undercurrent evolution recorded on Eirik Drift during the late Pliocene intensification of Northern Hemisphere Glaciation. Quat. Sci. Rev. 209, 40–51.

Blott, S.J., Pye, K., 2001. Gradistat: a grain size distribution and statistics package for the analysis of unconsolidated sediments. Earth Surf. Process. Landf. 26, 1237–1248.

Dausmann, V., Frank, M., Gutjahr, M., Rickli, J., 2017. Glacial reduction of AMOC strength and long-term transition in weathering inputs into the Southern Ocean since the mid-Miocene: evidence from radiogenic Nd and Hf isotopes. Paleoceanography 32, 265–283.

Day, R., Fuller, M., Schmidt, V., 1977. Hysteresis properties of titanomagnetites: grain-size and compositional dependence. Phys. Earth Planet. Inter. 13, 260–267.

de Carvalho Ferreira, M.L., Kerr, R., 2017. Source water distribution and quantification of North Atlantic Deep Water and Antarctic Bottom Water in the Atlantic Ocean. Prog. Oceanogr. 153, 66–83.

DePaolo, D.J., Maher, K., Christensen, J.N., McManus, J., 2006. Sediment transport time measured with u-series isotopes: results from ODP North Atlantic drift site 984. Earth Planet. Sci. Lett. 248, 394–410.

Droxler, A.W., Jorry, S.J., 2021. The origin of modern atolls: challenging Darwin's deeply ingrained theory. Annu. Rev. Mar. Sci. 13, 537–573.

Dunlop, D.J., 2002. Theory and application of the Day plot (Mrs/Ms versus Hcr/Hc) 2. Application to data for rocks, sediments, and soils. J. Geophys. Res. Solid Earth 107 (B3). EPM-5.

Egli, R., 2013. Variforc: an optimized protocol for calculating non-regular first-order reversal curve (FORC) diagrams. Glob. Planet. Chang. 110, 302–320.

Eldrett, J.S., Harding, I.C., Wilson, P.A., Butler, E., Roberts, A.P., 2007. Continental ice in Greenland during the Eocene and Oligocene. Nature 446, 176–179.

Faugères, J.C., Mézerais, M.L., Stow, D.A., 1993. Contourite drift types and their distribution in the North and South Atlantic Ocean basins. Sediment. Geol. 82 (1–4), 189–203.

Farmer, A., Rye, R., Landis, G., Bern, C., Kester, C., Ridley, I., 2003. Tracing the pathways of neotropical migratory shorebirds using stable isotopes: a pilot study. Isot. Environ. Health Stud. 39, 169–177.

Gruetzner, J., Higgins, S., 2010. Threshold behavior of millennial scale variability in deep water hydrography inferred from a 1.1 ma long record of sediment provenance at the Southern Gardar Drift. Paleoceanography 25.

Harrison, R.J., Feinberg, J.M., 2008. Forcinel: an improved algorithm for calculating first- order reversal curve distributions using locally weighted regression smoothing. Geochem. Geophys. Geosyst. 9.

Hassold, N., Rea, D., Van der Pluijm, B., Pares, J., Gleason, J., Ravelo, A., 2006. Late Miocene to Pleistocene paleoceanographic records from the Feni and Gardar drifts: pliocene reduction in abyssal flow. Palaeogeogr. Palaeoclimatol. Palaeoecol. 236, 290–301.

Hatfield, R.G., Stoner, J.S., Carlson, A.E., Reyes, A.V., Housen, B.A., 2013. Source as a controlling factor on the quality and interpretation of sediment magnetic records from the northern North Atlantic. Earth Planet. Sci. Lett. 368, 69–77.

Hatfield, R.G., Stoner, J.S., Reilly, B.T., Tepley III, F.J., Wheeler, B.H., Housen, B.A., 2017. Grain size dependent magnetic discrimination of Iceland and South Greenland terrestrial sediments in the northern North Atlantic sediment record. Earth Planet. Sci. Lett. 474, 474–489.

Hatfield, R.G., Wheeler, B.H., Reilly, B.T., Stoner, J.S., Housen, B.A., 2019. Particle size specific magnetic properties across the Norwegian-Greenland seas: Insights into the influence of sediment source and texture on bulk magnetic records. Geochem. Geophys. Geosyst. 20, 1004–1025.

Hayashi, T., Ohno, M., 2021. Diatoms in upper Pliocene–lower Pleistocene sediments, subpolar North Atlantic: 3. Thalassionema bacillare. Diatom 37, 22–29.

Hemming, S., Broecker, W., Sharp, W., Bond, G., Gwiazda, R., McManus, J., Klas, M., Hajdas, I., 1998. Provenance of Heinrich layers in core v28-82, northeastern Atlantic: $^{40}Ar/^{39}Ar$ ages of ice-rafted hornblende, Pb isotopes in feldspar grains, and Nd–Sr–Pb isotopes in the fine sediment fraction. Earth Planet. Sci. Lett. 164, 317–333.

Hergert, W., Wriedt, T., 2012. The Mie Theory: Basics and Applications, Vol. 169. Springer.

Hodell, D.A., Channell, J.E., 2016. Mode transitions in Northern Hemisphere glaciation: co-evolution of millennial and orbital variability in Quaternary climate. Climate of the Past 12 (9), 1805–1828.

Hodell, D.A., Evans, H.F., Channell, J.E., Curtis, J.H., 2010. Phase relationships of North Atlantic ice-rafted debris and surface-deep climate proxies during the last glacial period. Quat. Sci. Rev. 29, 3875–3886.

Jakobsson, S.P., 1972. Chemistry and distribution pattern of recent basaltic rocks in Iceland. Lithos 5, 365–386.

Jansen, E., Sjøholm, J., 1991. Reconstruction of glaciation over the past 6 myr from ice-borne deposits in the Norwegian sea. Nature 349, 600–603.

Kalsbeek, F., Taylor, P.N., 1985. Isotopic and chemical variation in granites across a Proterozoic continental margin—the Ketilidian mobile belt of South Greenland. Earth Planet. Sci. Lett. 73, 65–80.

Kanamatsu, T., Ohno, M., Acton, G., Evans, H., Guyodo, Y., 2009. Rock magnetic properties of the Gardar drift sedimentary sequence, site IODP U1314, North Atlantic: implications for bottom current change through the mid-Pleistocene. Mar. Geol. 265, 31–39.

Kissel, C., 2005. Magnetic signature of rapid climatic variations in glacial North Atlantic, a review. Compt. Rendus Geosci. 337, 908–918.

Kissel, C., Laj, C., Labeyrie, L., Dokken, T., Voelker, A., Blamart, D., 1999. Rapid climatic variations during marine isotopic stage 3: magnetic analysis of sediments from Nordic seas and North Atlantic. Earth Planet. Sci. Lett. 171, 489–502.

Kissel, C., Laj, C., Mulder, T., Wandres, C., Cremer, M., 2009. The magnetic fraction: a tracer of deep-water circulation in the North Atlantic. Earth Planet. Sci. Lett. 288, 444–454.

Kleiven, H.F., Jansen, E., Fronval, T., Smith, T., 2002. Intensification of Northern Hemisphere Glaciations in the circum Atlantic region (3.5–2.4 ma)–ice-rafted detritus evidence. Palaeogeogr. Palaeoclimatol. Palaeoecol. 184, 213–223.
Krissek, L.A., 1995. In: Rea, D.K., Basov, I.A., Scholl, D.W., Allan, J.F. (Eds.), in Proc. ODP, Sci. Results, 145. Ocean Drilling Program, College Station, Texas, pp. 179–194.
Larsen, H.C., Saunders, A.D., Clift, P.D., Beget, J., Wei, W., Spezzaferri, S., 1994. Seven million years of glaciation in Greenland. Science 264 (5161), 952–955.
Lisiecki, L.E., Raymo, M.E., 2007. Plio–pleistocene climate evolution: trends and transitions in glacial cycle dynamics. Quat. Sci. Rev. 26, 56–69.
Maslin, M., Li, X., Loutre, M.F., Berger, A., 1998. The contribution of orbital forcing to thep rogressive intensification of Northern Hemisphere Glaciation. Quat. Sci. Rev. 17, 411–426.
McCave, I., Manighetti, B., Robinson, S., 1995. Sortable silt and fine sediment size/composition slicing: parameters for palaeocurrent speed and palaeoceanography. Paleoceanography 10, 593–610.
Miller, K.G., Browning, J.V., Schmelz, W.J., Kopp, R.E., Mountain, G.S., Wright, J.D., 2020. Cenozoic sea-level and cryospheric evolution from deep-sea geochemical and continental margin records. Science advances 6 (20), eaaz1346.
Paterson, G.A., Zhao, X., Jackson, M., Heslop, D., 2018. Measuring, processing, and analyzing hysteresis data. Geochem. Geophys. Geosyst. 19, 1925–1945.
Prins, M.A., Bouwer, L.M., Beets, C.J., Troelstra, S.R., Weltje, G.J., Kruk, R.W., Kuijpers, A., Vroon, P.Z., 2002. Ocean circulation and iceberg discharge in the glacial North Atlantic: Inferences from unmixing of sediment size distributions. Geology 30, 555–558.
Raymo, M., Ruddiman, W., Backman, J., Clement, B., Martinson, D., 1989. Late Pliocene variation in northern hemisphere ice sheets and North Atlantic deep-water circulation. Paleoceanography 4, 413–446.
Raymo, M., Hodell, D., Jansen, E., 1992. Response of deep ocean circulation to initiation of Northern Hemisphere Glaciation (3–2 ma). Paleoceanography 7, 645–672.
Rohling, E.J., Foster, G.L., Grant, K.M., Marino, G., Roberts, A.P., Tamisiea, M.E., Williams, F., 2014. Sea-level and deep-sea-temperature variability over the past 5.3 million years. Nature 508 (7497), 477–482.
Ruddiman, W., 1977. North Atlantic ice-rafting: a major change at 75,000 years before the present. Science 196, 1208–1211.
Sato, M., Makio, M., Hayashi, T., Ohno, M., 2015. Abrupt intensification of North Atlantic Deep Water formation at the Nordic Seas during the late Pliocene climate transition. Geophys. Res. Lett. 42 (12), 4949–4955.
Schilling, J., Meyer, P., Kingsley, R., 1982. Evolution of the Iceland hotspot. Nature 296, 313–320.
Shackleton, N.J., Backman, J., Zimmerman, H.T., Kent, D.V., Hall, M., Roberts, D.G., Schnitker, D., Baldauf, J., Desprairies, A., Homrighausen, R., et al., 1984. Oxygen isotope calibration of the onset of ice-rafting and history of glaciation in the North Atlantic region. Nature 307, 620–623.
Snowball, I., Moros, M., 2003. Saw-tooth pattern of North Atlantic current speed during Dansgaard-Oeschger cycles revealed by the magnetic grain size of Reykjanes Ridge sediments at 59 N. Paleoceanography 18 (2).
Stickley, C.E., St John, K., Koc, N., Jordan, R.W., Passchier, S., Pearce, R.B., Kearns, L.E., 2009. Evidence for middle Eocene Arctic Sea ice from diatoms and ice-rafted debris. Nature. 460, 376–379.
Stoner, J.S., Channell, J.E., Hillaire-Marcel, C., 1995. Magnetic properties of deep-sea sediments off Southwest Greenland: evidence for major differences between the last two deglaciations. Geology 23, 241–244.
Tripati, A., Darby, D., 2018. Evidence for ephemeral middle Eocene to early Oligocene Greenland glacial ice and Pan-Arctic Sea Ice. Nat. Commun. 9, 1–11.
Ward, P.L., 1971. New interpretation of the geology of Iceland. Geol. Soc. Am. Bull. 82, 2991–3012.
Wilson, D.J., Bertram, R.A., Needham, E.F., van de Flierdt, T., Welsh, K.J., McKay, R.M., Mazumder, A., Riesselman, C.R., Jimenez-Espejo, F.J., Escutia, C., 2018. Ice loss from the East Antarctic ice sheet during late Pleistocene interglacials. Nature 561, 383–386.
Wold, C.N., 1994. Cenozoic sediment accumulation on drifts in the northern North Atlantic. Paleoceanography 9 (6), 917–941.